

Definition of an Uptake Pharmacophore of the Serotonin Transporter Through 3D-QSAR Analysis

J. Pratuangdejkul^{1,2,+}, B. Schneider³, P. Jaudon⁴, V. Rosilio⁵, E. Baudoin⁶, S. Loric⁷, M. Conti⁸, J-M. Launay^{1,2} and P. Manivet^{*,1,2}

¹Service de Biochimie et de Biologie Moléculaire, IFR 139, Hôpital Lariboisière, 2, rue Ambroise Paré, 75475 Paris Cedex 10, France

²E.A. 3621, Laboratoire de Biologie Cellulaire, UFR des Sciences Pharmaceutiques et Biologiques, 4 Avenue de l'Observatoire, 75006 Paris, France

⁺On leave from, Department of Microbiology, Faculty of Pharmacy, Mahidol University, Bangkok, Thailand

³Différenciation Cellulaire et Prions, CNRS UPR 1983, Institut André Lwoff, 7, rue Guy Môquet, 94801, Villejuif, and Institut Pasteur, Département de Biologie Cellulaire et Infections, Paris, France

⁴Université Paris-Sud. I.C.M.M.O. Laboratoire de Chimie Structurale Organique. Bat. 410. 91405 ORSAY Cedex, France

⁵Physicochimie des surfaces, UMR 8612 CNRS, Université Paris-Sud, rue J-B Clement, 92296 Chatenay-Malabry Cedex, France

⁶BioQuanta, 5, rue de l'Abbé de l'Épée, 75005 Paris, France

⁷Laboratoire de Biochimie-Génétique, Hôpital Henri Mondor, 51, rue du Maréchal de Lattre de Tassigny, 94010 Créteil, France

⁸Service de Biochimie 1, Hôpital Bicêtre, 78, rue du Général Leclerc, 94275 le Kremlin-Bicêtre Cedex, France

Abstract: The serotonergic system plays a critical role in a wide variety of physiological and behavioral processes. Dysregulation of the tightly controlled extracellular concentration of serotonin (5-hydroxytryptamine, 5-HT) appears to be at the origin of a host of metabolic and psychiatric disorders. Since the plasma membrane 5-HT transporter (SERT) is the major protagonist in regulating extracellular 5-HT concentration, SERT is the target of most drugs interacting with the serotonergic system. Unfortunately, some of the drugs towards SERT (e.g. amphetamine derivatives) interfere with cell homeostasis leading to cell toxicity. Developing new SERT ligands devoid of any side-effect represents a major priority in the treatment of 5-HT-associated pathologies. Here, we report structure-activity relationships (SAR) and three-dimensional QSAR (3D-QSAR) studies of a library of 121 compounds including 5-HT analogs, harmanes, benzothiazoles, indanones, amphetamine derivatives and substrate-type 5-HT releasers, with the goal of identifying the structural determinants crucial for SERT uptake. In the absence of data about the bioactive form of 5-HT, conformational analysis of 5-HT was performed using quantum chemistry calculations. This led to three 5-HT stable conformers with *anti*, *-gauche* and *+gauche* side-chain conformation. These conformers, used as templates for superimposition with all the library compounds, enabled the design of a reliable 6-points pharmacophore representative of SERT uptake activity. Molecular dynamics (MD) simulations performed with compounds that are efficiently, moderately, poorly or not transported by SERT allowed to assess the validity of our pharmacophore. Altogether, our data provide for the first time a reliable pharmacophore of SERT uptake activity, which may help to the design of new drugs targeting SERT.

Keywords. SERT, serotonin transporter, 5-HT, 5-hydroxytryptamine, 3D, three-dimensional, QSAR, quantitative structure-activity relationships, pharmacophore.

INTRODUCTION

The monoamine serotonin (5-hydroxytryptamine, 5-HT) controls a wide variety of physiological and behavioral processes, including sleep, anxiety and cognition as well as memory or perception [1]. A key step that determines the intensity and duration of 5-HT signaling is the re-uptake of extracellular 5-HT into cells through the 5-HT transporter

(SERT). SERT belongs to the super family of Na⁺/Cl⁻-dependent transporters [2, 3] and assumes the transport of extracellular 5-HT across the cell membrane of neurons, gut enterochromaffin cells and platelets. Uptake of 5-HT by SERT is electroneutral, *i.e.* 5-HT is co-transported with Na⁺ and Cl⁻ ions, and is counter-transported with K⁺ ion [4]. Because SERT plays a fundamental role in regulating extracellular 5-HT, therapeutic strategies have mainly focused on the development of compounds that block the function of SERT. For instance, a large panel of drugs, including abuses drugs and therapeutic drugs prescribed for the treatment of many psychiatric disorders and metabolic

*Address correspondence to this author at the Service de Biochimie et de Biologie Moléculaire, Hôpital Lariboisière, 2, rue Ambroise Paré, 75475 Paris Cedex 10, France; Tel: 33-1-49956432; E-mail: crcb.manivet@lrh.ap-hop-paris.fr

diseases, has been synthesized (for review, see [5]). Drugs that target SERT can be divided into two major classes: reuptake inhibitors and substrate-type releasers. Reuptake inhibitors (tricyclics, SSRIs) bind to SERT molecules, but are not themselves transported. By contrast, substrate-type releasers (e.g. amphetamines) bind to SERT and are subsequently transported across the plasma membrane. Releasers elevate extracellular 5-HT concentration by a two-pronged mechanism: (i) they promote efflux of transmitter by a process of transporter-mediated exchange and (ii) they induce exocytosis of transmitter storage vesicles.

It is interesting to note that some of the drugs targeting SERT, like amphetamine derivatives, are toxic, thus increasing the risk of valvular heart disease and of developing primary pulmonary hypertension (for review, see [6]). It is of a matter of fact that the characterization of transmitter and ions molecular transport processes through SERT is important to design new generations of optimized SERT inhibitors. These lead-optimizations usually rely on structural informations concerning the SERT molecule. Unfortunately, no three-dimensional (3D) structure has yet been solved for any transporters belonging to the super family of Na⁺/Cl⁻-dependent transporters. Based on the hydropathy scoring method, putative topological models for Na⁺/Cl⁻-dependent transporters have predicted a total of 12 transmembrane-spanning domains (TMDs), connected by six extracellular and five cytoplasmic loops, with both the N- and C-terminal ends plunged into the cytosol (for review, see [7]). The identification of amino acids involved in ligand binding as well as in the transport process were previously assessed by site-directed mutagenesis [8-27]. Nevertheless, 3D models of bioamine transporters have been built using homology modeling techniques. The first 3D model of a monoamine transporter concerns the dopamine transporter (DAT) [28]. Recently, new 3D models of DAT, as well as structural models of SERT, and norepinephrine transporter (NET) have been proposed [29-31]. For instance, the low homology between the primary sequences of SERT and of *Escherichia coli* Na⁺/H⁺ antiporter (NhaA) [32] used as template for modeling as well as their far-related mechanism of transport, have weakened the accuracy of the proposed 3D models for SERT. Mutagenesis, biophysical and functional experiments are further needed to improve those 3D models.

In absence of reliable 3D data on the targeted macromolecule, another option to get structural information consists in determining the structural activity relationships (SAR) of a compound library and further, in defining a pharmacophore of transport. SAR analysis previously performed with 5-HT analogs led only to two-dimensional SAR models [33-37]. Besides, these SAR models are the definition of a pharmacophore of inhibition of monoamine transporters, since they were designed using a library of non-transported compounds [38-42].

From a 121 synthetic compound library, we utilized all 5-HT analogs, that displayed the highest SERT-associated transport activity, to define a pharmacophore of SERT uptake. We measured the uptake of each compound through SERT using human blood platelets, a relevant model for investigating 5-HT transport [43, 44]. In addition, we established, *in silico*, quantitative structure-activity relationships (QSAR) of the initial compound library, in

order to define the physicochemical properties of molecules transported through SERT.

As no reliable information is available for the right bioactive conformation of any compounds, we first identified stable conformations of 5-HT by quantum chemistry calculations, which were used as reference conformers in alignment protocols with the library compounds. Second, we generated a 3D-QSAR model of SERT transport activity, which allowed to define a reliable pharmacophore of drug uptake. Finally, we proposed that our pharmacophore of "activity" and our 3D-QSAR model may find applications in 3D-database search, data mining, prediction of uptake activity for other compounds or may provide basic informations for SERT modeling.

MATERIALS AND METHODS

Experimental Procedures

Platelets Isolation and Preparation

Platelets were isolated from fresh blood samples (anticoagulant : ACD-A *i.e.* citric acid 11.9 g/L, anhydrous trisodium citrate 32.6 g/L, dextrose 36.3 g/L; 1v/9v) collected between 8 and 10 a.m. from a unique fasting adult Caucasian man (JML, age 33 years), who did not suffer from either acute or chronic diseases. He did not receive either 5-HT- or tryptophan-rich food for the last two days or any medication during three weeks prior blood collection. The isolation and preparation of intact platelets were carried out at room temperature by iterative centrifugations [45]. Platelets were counted by contrast-phase microscopy before and after the isolation procedure. Platelet activation was detected by the reduced ability of platelets to aggregate (Chronolog whole blood aggregometer, Beckman-Coulter France SA) upon stimulation with ADP (1 μM). Only non activated isolated platelets were selected for further experiments.

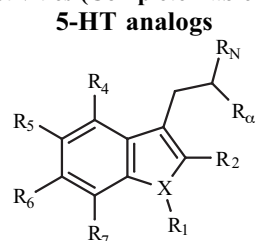
SERT Uptake Assay

Uptake of 5-HT binoxalate or of any chemical analogs (10⁻⁵ M) into isolated human platelets was measured within a 60s time scale as previously described in [46], in Tyrode-Tris buffer, pH 7.40, 290-310 mOsm/L (NaCl, 130 mM; KCl, 5.6 mM; Tris, 12.4 mM; Na₄EDTA, 2.1 mM; Na H₂PO₄, 0.9 mM; sucrose, 13.1 mM; and dextrose, 11.1 mM) modified from Gadd and Clayman (1972) [47]. The amount of transported compound was measured by spectrofluorometry (Aminco-Bowman apparatus) with λ_{exc} between 260 and 455 nm and λ_{em} between 340 and 540 nm, depending on the tested compound. The amount of endogenous 5-HT within platelets and possibly released by each compound was also taken into account, since this might constitute a bias [48].

Compound Library

QSAR studies were performed using a focused library of 121 chemical analogs of 5-HT including harmanes, benzothiazoles, indanones, amphetamine derivatives and substrate-type 5-HT releasers. Some of these compounds were reagent grade, purchased from commercial sources.

Table 1. Chemical Structures and SERT Uptake Activities (Complete Table Available on Request)

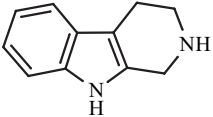
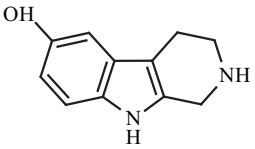
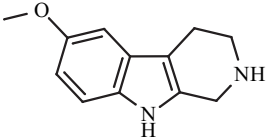
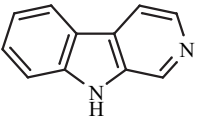
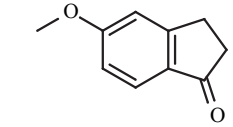
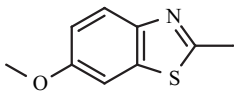
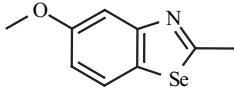


Training set for QSAR models										
Compound	X	R ₁	R ₂	R ₄	R ₅	R ₆	R ₇	R _α	R _N	Uptake ^(a)
1	N	H	H	H	OH	H	H	H	NH ₃ ⁺	13.31 ± 0.27
2	N	H	H	H	OH	H	H	H	NH ₂ ⁺ (CH ₃)	9.87 ± 0.12
3	N	H	H	H	OH	H	H	CH ₃	NH ₃ ⁺	9.21 ± 0.05
4	N	H	H	H	OH	H	H	H	NH ⁺ (CH ₃) ₂	3.75 ± 0.64
5	N	H	H	H	OH	H	OCH ₃	H	NH ₃ ⁺	1.84 ± 0.09
6	N	H	H	H	OH	H	OH	H	NH ₃ ⁺	1.66 ± 0.04
7	N	H	H	H	OH	H	H	COO ⁻	NH ₃ ⁺	1.15 ± 0.08
8	S	-	H	H	OH	H	H	H	NH ₃ ⁺	0.98 ± 0.23
9	C	H,H	H	H	OH	H	H	H	NH ₃ ⁺	0.94 ± 0.10
10	N	H	H	H	H	H	H	COO ⁻	NH ₃ ⁺	0.91 ± 0.27
11	N	H	H	H	OH	OH	H	H	NH ₃ ⁺	0.79 ± 0.05
12	N	H	H	H	OH	OCH ₃	H	H	NH ₃ ⁺	0.77 ± 0.09
13	N	H	H	OH	H	H	H	H	NH ₃ ⁺	0.68 ± 0.02
14	N	H	H	H	H	H	OH	H	NH ₃ ⁺	0.50 ± 0.09
15	N	H	H	H	H	OH	H	H	NH ₃ ⁺	0.49 ± 0.10
16	N	H	H	H	H	H	H	H	NH ₃ ⁺	0.48 ± 0.03
17	C	H,H	H	H	H	H	H	H	NH ₃ ⁺	0.47 ± 0.10
18	N	H	H	H	OH	OH	OH	H	NH ₃ ⁺	0.43 ± 0.05
19	N	H	H	H	OCH ₃	OH	H	H	NHCO(CH ₃)	0.42 ± 0.11
20	N	H	H	H	H	F	H	COO ⁻	NH ₃ ⁺	0.40 ± 0.05
21	N	CH ₃	H	H	H	H	H	H	NH ₃ ⁺	0.33 ± 0.05
22	N	CH ₃	H	H	H	H	H	COO ⁻	NH ₃ ⁺	0.28 ± 0.05
23	C	H,H	H	H	H	H	H	COO ⁻	NH ₃ ⁺	0.25 ± 0.08
24	N	H	H	H	H	H	H	H	NH ₂ ⁺ (CH ₃)	0.23 ± 0.02
25	N	H	H	H	OH	H	H	H	NHCO(CH ₃)	0.21 ± 0.06
26	N	CH ₃	H	H	H	H	H	H	NH ₂ ⁺ (CH ₃)	0.19 ± 0.02
27	N	H	H	H	OCH ₃	H	H	H	NH ₃ ⁺	0.15 ± 0.02
28	N	H	H	H	H	H	H	H	NHCO(CH ₃)	0.13 ± 0.03
29	N	H	H	H	H	H	H	COO ⁻	NHCO(CH ₃)	0.12 ± 0.04
30	N	H	H	H	OCH ₃	H	H	H	NHCO(CH ₃)	0.12 ± 0.03
31	S	-	H	H	H	H	H	H	NH ₃ ⁺	0.08 ± 0.03
32	N	CH ₃	H	H	H	H	H	H	NH ⁺ (CH ₃) ₂	0.07 ± 0.06
33	N	H	H	H	H	H	H	H	NH ⁺ (CH ₃) ₂	< 0.05
34	N	H	H	H	H	OCH ₃	H	H	NH ₃ ⁺	< 0.05
35	N	H	H	H	OCH ₃	H	H	H	NH ⁺ (CH ₃) ₂	< 0.05

(Table 1). contd.....

Training set for QSAR models										
Compound	X	R ₁	R ₂	R ₄	R ₅	R ₆	R ₇	R _α	R _N	Uptake ^(a)
36	N	H	H	H	OCH ₃	H	H	CH ₃	NH ₃ ⁺	< 0.05
37	N	H	H	H	H	OH	H	H	NHCO(CH ₃)	< 0.05
38	N	H	H	H	H	OCH ₃	H	H	NHCO(CH ₃)	< 0.05
39	S	-	H	H	H	H	H	H	NH ₂ ⁺ (CH ₃)	< 0.05
40	S	-	H	H	H	H	H	H	NH ⁺ (CH ₃) ₂	< 0.05
41	O	-	H	H	H	H	H	COO ⁻	NH ₃ ⁺	< 0.05
42	N	H	H	H	OH	H	H	OH	H	< 0.05
43	N	H	H	H	OCH ₃	H	H	OH	H	< 0.05
44	N	H	H	H	OH	H	H	COO ⁻	H	< 0.05
45	N	H	H	H	OH	H	H	COO ⁻	OH	< 0.05
46	N	H	H	H	OCH ₃	H	H	COO ⁻	NH ₃ ⁺	< 0.05
External test set										
47	N	H	H	H	OH	F	H	H	NH ₃ ⁺	2.30 ± 0.02
48	N	H	H	F	OH	F	H	H	NHCO(CH ₃)	0.84 ± 0.07
49	N	H	H	F	OH	F	H	H	NH ₃ ⁺	0.37 ± 0.09
50	N	H	H	F	OCH ₃	F	H	H	NH ₃ ⁺	0.28 ± 0.02
51	N	H	H	H	OH	F	H	H	NHCO(CH ₃)	0.23 ± 0.03
52	N	H	H	H	F	H	H	COO ⁻	NH ₃ ⁺	0.17 ± 0.06
53	N	H	H	H	H	F	H	H	NH ₃ ⁺	0.16 ± 0.04
Non-included compounds in QSAR models										
56	N	H	H	H	OCH ₃	OCH ₃	H	H	NHCO(CH ₃)	< 0.05
57	N	H	H	H	OCH ₃	H	OCH ₃	H	NH ₂ ⁺ (CH ₃)	< 0.05
58	N	H	H	H	OCH ₃	H	OCH ₃	H	NH ₂ ⁺ C ₂ H ₅	< 0.05
59	N	H	H	H	OCH ₃	H	OCH ₃	H	NH ⁺ (C ₂ H ₅) ₂	< 0.05
60	N	H	H	H	OCH ₃	OCH ₃	OCH ₃	H	NH ⁺ (CH ₃) ₂	< 0.05
61	N	H	H	OCH ₃	H	H	H	H	NH ₃ ⁺	< 0.05
62	N	H	H	OCH ₃	H	H	H	H	NH ⁺ (CH ₃) ₂	< 0.05
63	N	H	H	H	H	OCH ₃	H	H	NH ⁺ (CH ₃) ₂	< 0.05
64	N	H	H	H	H	H	OCH ₃	H	NH ₂ ⁺ C ₂ H ₅	< 0.05
65	N	H	H	H	H	H	H	C ₂ H ₅	NH ₃ ⁺	< 0.05
68	N	H	H	H	NH ₂	H	H	H	NH ₃ ⁺	< 0.05
69	N	H	H	H	CH ₃	H	H	H	NH ₃ ⁺	< 0.05
70	N	H	H	H	F	H	H	H	NH ₃ ⁺	< 0.05
74	N	H	H	H	OSO ₃ ⁻	H	H	H	NH ₃ ⁺	< 0.05
75	S	-	H	H	H	H	H	COO ⁻	NH ₃ ⁺	< 0.05
78	O	-	H	H	OH	H	H	H	NH ₃ ⁺	< 0.05
80	N	H	H	H	OH	H	H	H	NH-galactose	< 0.05
81	N	H	H	H	OH	H	H	H	NH-fucose	< 0.05
82	N	H	H	H	OH	H	H	H	NH-ribose	< 0.05
83	N	H	H	H	OH	H	H	H	NH-fructose	< 0.05
87 ^(b)	N	H	H	H	OH	H	H		H (no side chain)	< 0.05

(Table 1). contd....

Non-included compounds in QSAR models		
Compound (c)	Structure	Uptake(a)
109		< 0.05
110		< 0.05
111		< 0.05
112		< 0.05
113		< 0.05
114		< 0.05
115		< 0.05

(a) SERT-uptake activity is expressed in nmole/10⁹ platelets (mean ± standard error of mean, n = 4)

(b) compound 87 is 5-hydroxyindole

(c) compounds 109-115 are harmanes, benzothiazoles and indanones derivatives.

Others were generous gifts from Roche (Basel), Upjohn (Kalamazoo), Pr L. Mester (ICSN, CNRS, Gif-sur-Yvette), Drs A. Manian, P.J. Marangos, S.P. Markey (NIH, Bethesda), T.R. Bosin, D.E. Mais (Indiana University, Bloomington), and A.H. Drummond (University of Glasgow). Uptake by human platelet SERT was assessed for each compound as described above (Table 1). To further evaluate the predictive power of derived QSAR models, a set of 5-HT analogs (Table 1), substrate-type 5-HT releasers and related compounds [6] (see Fig. (1)), were used as an external test set.

Computational Procedures

Molecular Modeling

Molecular modeling protocols were performed on a Silicon Graphics O₂ R12000 workstation running under the IRIX 6.5 operating system. Structures of all compounds were built using the Biopolymer module included in the

InsightII molecular modeling package (Molecular Simulations Inc., San Diego, CA). Energy calculations and molecular dynamics (MD) simulations were performed using the CHARMM molecular mechanics package [49]. Carboxyl and amine groups were considered ionized, in order to respect their ionization state at physiological pH [50]. All compounds of the library were submitted to MD simulations in water at 300 K: i) each compound was hydrated in equilibrated boxes (25 x 25 x 25 Å) of 465 molecules of TIP3P water [51]; the box was replicated with periodic boundary conditions. The non-bonded list was cut off at 10 Å, and, ii) simulations were then performed according to the following protocol: energy minimizations were carried out with the Steepest Descent and Adopted Basis set Newton-Raphson routines to rms gradients < 10⁻⁴ kcal mol⁻¹ Å⁻¹; the energy-minimized systems were heated at 300 K during 6 picoseconds (ps) and equilibrated during 50 ps; production was performed in the microcanonical ensemble for 500 ps; bond lengths were constrained with the SHAKE algorithm [52] and the integration time step was 1 fs.

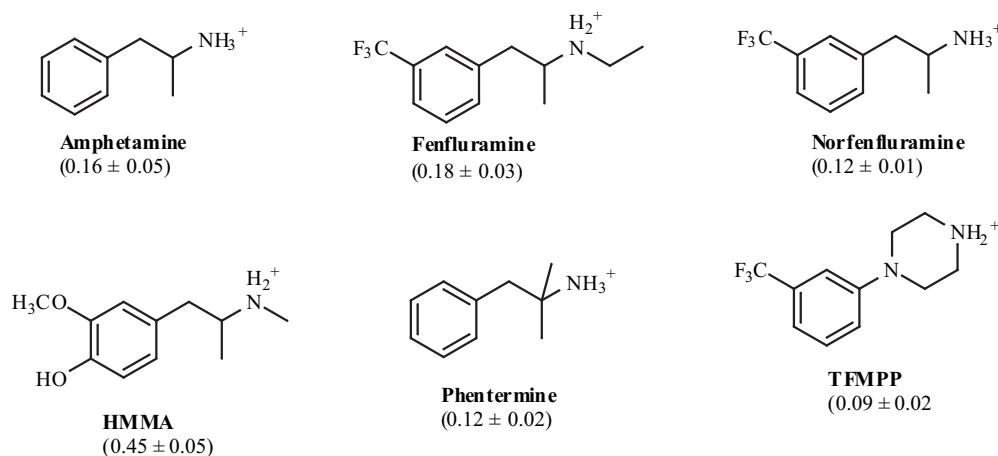


Fig. (1). Chemical structures and SERT-uptake activities in nmole/10⁹ platelets (mean ± standard error of mean, n = 4) of substrate-type 5-HT releasing agents and related compounds used as external test set. HMMA: 4-hydroxy-3-methoxymethamphetamine, TFMPP: m-trifluoromethylpiperazine.

For all theoretical calculations, 5-HT was chosen as the reference molecule since it represents the physiological compound primarily SERT transported. Nevertheless, since there is no information available for the 5-HT bioactive conformation, an adiabatic conformational analysis of 5-HT was performed by systematically rotating dihedral angles of the ethylamine side chain. All calculations were carried out using the Gaussian03 package of programs [53]. The conformational analysis was performed at the B3LYP/6-31+G(d,p) level of theory. At each angle increment, the geometry of the molecule was relaxed and fully optimized. All geometry optimizations were done without any symmetry constraints in order to avoid bias that could impose a particular symmetry to 5-HT structures. Local-energy minima (no imaginary frequencies) were then used as rigid reference templates for molecule alignments. This above protocol (adiabatic conformational analysis) was also repeated for all library compounds in order to generate a new set of CHARMM parameters specific of each 5-HT derivative. For individual compound, CHARMM partial charges were then adjusted to obtain dipole moments comparable to those derived from quantum chemistry calculations.

Superposition Technique

The 121 compounds belonging to our library were aligned to 5-HT using FLEXS program [54]. For this process, predefined informations that relate to the pharmacophore shared by the reference and library molecules were not required [54-56]. Steric and hydrogen bond pattern options were selected as superposition parameters for fitting procedures. A standard algorithm, based on geometric hashing and volume overlap optimization [57], was used to superpose tested molecules onto the reference one. Since electrostatic interactions are critical for this superposition process, the set of optimized partial charges (see above) was thus considered to obtain reliable conformers. A fitting score was attributed to each conformer, which was used to rank all library molecules. For each tested compound, 30 conformers with the highest fitting score were energy minimized with Steepest Descent and Adopted basis set Newton-Raphson

methods included in the CHARMM program. Accordingly, we eliminated non reliable conformers exhibiting high energy values as well as conformers evolving toward the nearest local minimum.

Classical QSAR

To find a relationship between SERT uptake activity and chemical structures of all compounds, we first performed a classical QSAR analysis. Using structures derived from the alignment procedure, we generated a set of physicochemical descriptors¹. All descriptors and analyses were computed with the TSAR 3.3 program package (Accelrys Inc, San Diego, CA). A statistical partial-least-square (PLS) analysis was carried out for all structures in order to establish a linear quantitative relationship between the dependent (uptake) and independent (calculated descriptors) variables.

In order to reduce bias in the building QSAR model, we reduced the number of non-transported compounds using PLS. Briefly, an initial QSAR model was built and iteratively refined to a maximum of predictability (maximum correlation coefficient r^2 , minimum standard error of prediction s) by eliminating redundant compounds and outliers, which introduced statistical noise. Only non transported compounds were eliminated one by one and the regression curve was re-plotted. Compounds with two standard deviations out of the regression curve were definitively removed.

Molecular Interaction Fields (MIFs) and Descriptors for 3D-QSAR

To gain insight into the relationship between the 3D structure of each compound and its transport through SERT, we applied the standard molecular interaction fields (MIFs) procedure calculation to all compounds. Non-bonded interaction energies between a compound and a probe were calculated using the GRID20 program [58]. Three probes were selected in this study: DRY (hydrophobic probe), O (O

¹Available upon request.

carbonyl probe), and N1 (N amide probe), which represent hydrophobic, hydrogen bond acceptor and hydrogen bond donor groups, respectively. Considering the surface mapping process, the setting parameters used were: 0.5 Å grid spacing, 100 extracted nodes, 30% weight of field importance and 0.8 smoothing window in order to obtain descriptors for each of three auto-correlogram (*i.e.* DRY-DRY, O-O, and N1-N1) and three cross-correlogram (*i.e.* DRY-O, DRY-N1, and O-N1) variable blocks.

From MIFs calculations, Grid Independent Descriptors (GRINDs) were coded using the ALMOND 2.0 software [59]. GRINDs represent alignment of independent descriptors in relation to the ability of each compound to establish favorable interactions with independent pharmacophoric groups. The grid nodes showing the energetically most favorable interactions with the probes were then selected. Distances between the selected nodes representing the same type of MIFs (auto-correlograms) or different types of MIFs (cross-correlograms) were calculated. GRINDs were thereafter generated by calculating the maximal energy value for each grid point pairs ("smoothing windows" option).

Statistical Analysis and Model Validation

To perform a statistically significant QSAR, the partial least square (PLS) methodology was used to analyze the relationship between generated descriptors and SERT uptake values. The cross-validation PLS calculation was performed using leave-one-out (LOO), and leave-five-out (LFO) random procedures. The non-cross-validated r^2 , cross-validated r^2 (expressed as q^2) correlation coefficients, and the standard error of prediction s were examined to assess the validity of all models. s values were calculated according to the equation $s = (\text{PRESS}/N)^{1/2}$, where $\text{PRESS} = \sum(\text{Predicted value} - \text{Experimental value})^2$ and N is the total number of compounds. Correlation coefficients of prediction for external test set, r^2_{PRED} values, were estimated according to the equation $r^2_{\text{PRED}} = (\text{SD}-\text{PRESS})/\text{SD}$, where SD is the sum of the squared deviations between the biological activities of the test set and mean activity of the training set [60]. The parameter r^2 enabled to appreciate how good is the correlation between experimental and predicted SERT uptake values. q^2 and s were representative of the predictability power of the proposed models.

The optimal numbers of components we used to derive our models were selected according to the internal predictive ability by the LOO cross-validation method. This procedure yielded the optimal number of PLS components, which were defined as the number of components leading to the highest cross-validation coefficient, q^2_{LOO} and the lowest standard error of prediction, s_{LOO} .

For the classical QSAR analysis, calculated descriptors were pre-treated using the "standardization by means" method implemented in TSAR. For 3D-QSAR analysis, calculated descriptors were pre-treated with the "normalize block-wise scaling" method before performing PLS analysis. First, each PLS model was generated using the optimal number of components as mentioned above. Some GRINDs were not relevant for precise description of the mode of interaction between ligands and SERT. In addition, these

irrelevant GRINDs introduced noise in the statistical PLS analysis [58]. We thus performed a "standard variable selection" with the help of the fractional factorial design (FFD) algorithm, which was also implemented in the ALMOND software (for a detailed description of this approach, see references [61-62]). In our study, FFD variable selection was performed using the following parameters: the optimal number of components and the LOO cross-validation method [63-65].

Pharmacophore Development

To grasp the relationship between chemically modified compound 3D structures, and SERT uptake activity, we defined a pharmacophore. With the three sets of compounds obtained after superposition with the three most stable conformers of 5-HT, a QSAR analysis was performed in order to select the most reliable model. With the help of compounds taken up by SERT, we identified key points, which were referenced as pharmacophoric centers. This pharmacophore for SERT uptake appeared as relevant since (i) it was deduced from the set of transported compounds, (ii) it contained the maximal number of pharmacophore component moieties, (iii) it exhibited the smallest total variances in the distance matrix and angle. MD simulations of the most transported and non-transported compounds, which referred to positive and negative controls, respectively, enabled us to control the validity of this pharmacophore. Transported compounds exhibited a high probability to adopt a conformation fitting with the pharmacophore along the molecular dynamics trajectory, while SERT could never accommodate the conformation of non-transported compounds.

RESULTS

Structure-Activity Relationships

We built a library of chemical analogs of 5-HT in order to investigate 5-HT uptake by SERT and to define a rational pharmacophore for this transporter. We derived our compound library from the 5-HT molecule by performing chemical substitutions, keeping the indole ring as reference. Substrate-type releasers were kept as external test set to control the validity of the 3D-QSAR models. SERT uptake activities of 121 analogs of 5-HT and substrate-type releasers were tested using human platelets. Nearly every compound selected for evaluation differed from another one taken in the series by a single structural modification. Chemical structures and 5-HT uptake values are listed in Table 1. We noticed that none of the examined compounds displayed significant higher uptake than 5-HT. Nevertheless, this library allowed to identify four different chemical zones within the 5-HT molecule, which are crucial for uptake by SERT. They include the cationic head, the 5-hydroxyl group, the indole nitrogen atom and the aromatic zone composed of the six-membered-ring.

In SERT, an aspartate residue was previously identified to be required for 5-HT uptake through interaction with the 5-HT cationic head [15]. Such contact is also well documented as being necessary to the binding process of 5-

HT to serotonin receptors [66-69]. We thus substituted the ammonium group of 5-HT with chemical groups exhibiting different sizes to appreciate the impact of the spatial hindrance of the substituted amine group on 5-HT-modified compound uptake by SERT. The substitution of the cationic head by methyl group (compounds **2** and **4**, Table 1), with respect of the positive charge of the ammonium group, moderately impacted on the uptake activity by SERT. Compounds **2** and **4** were transported with an efficacy of 75% and 30%, respectively, as compared to 5-HT. The introduction of acetamide or glycozylating groups at the R_N position (compounds **25**, **80-83**, Table 1), which both neutralized the cationic head and increased the steric hindrance of this side chain, altered SERT uptake activity by almost 100%. In addition, cyclizing the ethylamine side chain (harmaline compounds **109-112**, Table 1) both neutralized the charge of the cationic head and canceled the flexibility of this side chain. These combined effects abrogated SERT uptake capacity. However, it is interesting to note that the presence of a positive charge on the ethylamine side chain is more crucial for SERT uptake activity than the steric hindrance of this side chain. This was again supported when removing the ethylamine side chain (compound **87**), which totally abrogated compound uptake. Another option to appreciate the importance of the conformation of the cationic ethylamine side chain was to introduce a carboxyl group at the R_α position (compound **7**, Table 1). This induced a repulsive interaction between the negative charge of the carboxyl group and the π -electrons of the indole ring, which resulted in positioning the cationic ethylamine side chain in an extended conformation. The uptake efficacy for compound **7** decreased by 11-fold. This suggests that neutralizing the global charge within the derivative is less detrimental for SERT uptake activity than suppressing the positive charge of the ammonium group. Furthermore, this indicates that the derived cationic head of 5-HT side chain adopting an extended conformation fits the SERT binding site.

The hydroxyl group at the R_5 position was suspected to act as acceptor or donor of hydrogen bonds. Substitution of the R_5 -OH group by a hydrogen atom (compound **16**) dropped down compound uptake as compared to 5-HT. The molecule was still transported but rather weakly (3%). By contrast, compounds with either NH_2 (compound **68**), CH_3 (compound **69**), F (compound **70**), or OSO_3^- (compound **74**) chemical functions replacing the R_5 -OH group were never transported. As concerns modified compounds with a bulky methoxyl group at the R_5 position (compound **27**), we observed that this substitution has a larger impact on SERT-uptake activity than removing the OH group itself. In addition, modification of the R_5 -OH group by a methoxyl function in compounds **34**, **35**, **57** to **64** (Table 1), with respect of a positive charge on the cationic head, canceled uptake. Suppressing the positive charge of the cationic head in combination to the introduction of a methoxyl group at the R_6 position (compound **38**, Table 1) prevented uptake by SERT. Further addition of a methoxyl group at the R_5 position (compound **56**, Table 1) did not restore any uptake activity. These results clearly establish that the presence of a hydroxyl group at the R_5 position is required for efficient uptake by SERT. The steric hindrance due to the methoxyl group introduction is however deleterious for transport. This

suggests that the volume of the 5-HT binding site is adapted for hydroxyl group accommodation. We may also hypothesize that the methoxyl function alters the H-bond network surrounding the OH group, thus preventing the correct orientation of derivatives for efficient binding and/or transport.

To refine the SAR study and to start to dissect the topology of the putative binding site of SERT, we also shifted in compounds **13-15** the hydroxyl group from the R_5 position to the R_4 , R_7 or R_6 positions, respectively. Translocation of the hydroxyl group (compounds **13** to **15**) decreased the uptake by 20- to 30-fold as compared to 5-HT. We noticed that substitutions at R_6 and R_7 positions were more deleterious for SERT-uptake activity than the R_4 -OH modification.

We also designed molecules with multi-substitutions including several hydroxyl groups (homo-multi-substitutions) or bearing distinct chemical groups *i.e.* hydroxyl and methoxyl groups (hetero-multi-substitutions). With multi-hydroxylated compounds (**6**, **11** and **18**), uptake significantly dropped down 8-, 17-, and 31-fold, respectively using 5-HT as the reference molecule. The simultaneous introduction of two hydroxyl groups (compound **11**) led to a reduced uptake of nearly 17-fold. Further introduction of a third hydroxyl group (compound **18**) negatively impacted on uptake by 31-fold. Hetero-multi-substitutions (compounds **5** and **12**) had weaker incidence on SERT-uptake activity (uptake decreased by 7- and 17-fold, respectively) than shifting the hydroxyl group from R_5 to R_6 , R_7 or R_4 positions (compounds **13** to **15**) or than substituting R_5 -OH function by a methoxyl group (compound **27**). When comparing compounds **5** and **12**, we observed that SERT-uptake activity was much lower when the bulky methoxyl group was in the close vicinity of the R_5 -OH function.

Finally, substitutions at the R_α position by methyl or ethyl groups (compounds **36** and **65**, respectively, Table 1) in addition to the R_5 -OH modification also abolished uptake. Nevertheless, when a methyl group was the unique substitution performed at the R_α position (compound **3**, Table 1), the presence of all other key-chemical elements in the molecule was sufficient to compensate this unique modification. Indeed, a very slight decrease (1.5-fold) in SERT uptake activity was recorded. Again these results support the importance of the R_5 -OH group in the transport process.

The close examination of serotonin receptors in complex with 5-HT [69] strongly indicated that the indole nitrogen atom allows the optimal docking of 5-HT in the receptor binding site. When the indole nitrogen was thus substituted by sulfur (compound **8**) or carbon atoms (compound **9**), the derived molecules were transported by SERT with an efficiency that was almost 14-fold lower than the one of 5-HT. By contrast, replacement of the indole nitrogen atom by an oxygen atom (compound **78**) totally canceled the modified compound uptake by SERT. Modification of the indole nitrogen atom by either carbon or sulfur atoms in combination with the removal of the R_5 -OH group (compounds **17** and **31**, respectively) allowed to discriminate between carbon or sulfur modified compounds. Indeed, we observed that compound **17** was 6 times more efficiently transported than compound **31**, while parent compounds **8**

and **9** were transported with similar efficacies. Interestingly, compounds **16** and **17**, differing by the nitrogen to carbon substitution in the indole ring only, were SERT-transported with similar efficacies. Altogether, our data strongly support the view that indole nitrogen atom substitution by a carbon atom is the less deleterious modification in regards with SERT functionality.

The indole ring skeleton is a hallmark of all our library compounds. This canonical structure seems to be adapted to an optimal SERT uptake. Indeed, other aromatic structures that refer to molecules belonging to the benzothiazole compound **114** or indanone families compound **113**, failed to be transported by SERT (Table 1). An unanswered question was, however, to know whether the indole ring interacts with specific SERT residues. For instance, stacking or T-shape interactions between the 5-HT indole ring and SERT aromatic residues are suspected. We cannot exclude that the aromatic region of the SERT molecule might also interact with other chemical functions of 5-HT, leading to a favorable orientation of the neurotransmitter in the SERT binding site. This hypothesis is supported by the observation that compounds with no indole ring-shape (Fig. (1)) are indeed transported by SERT.

Finally, R_α carboxyl-induced extended conformation of the cationic ethylamine side chain in combination with any R₅ hydroxyl group substitution (compounds **10** and **20**, Table 1) reduced the uptake by 14- and 33-fold, respectively. Further substitutions of these latter derivatives differentially affected the uptake depending on the targeted key-zone: S substitution of the indole nitrogen atom (compound **75**, Table 1) abolished uptake; R_N substitution by an acetamide function (compound **30**, Table 1) drastically reduced uptake by 110-fold; R₁ substitution (compounds **22** and **23**, Table 1) diminished uptake by 45- and 53-fold, respectively.

From these overall data, we conclude that (i) any OH group substitution by a bulkier function is detrimental for uptake by SERT, and (ii) replacement of the nitrogen indole atom is deleterious for uptake when combined to any other

substitutions, whereas (iii) extended conformation of the cationic head side chain is important for uptake with respect of a positive charge on the ammonium group.

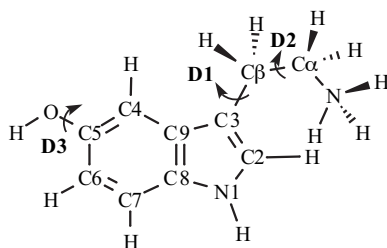
Conformational Analysis of 5-HT and Superposition of Compounds

One of the most important and sensitive step in 3D-QSAR studies is the superposition of candidate molecules on a reference one. Routinely, only one conformation, which corresponds to the lowest energy conformer of the reference template, is used for the molecule alignment process. Since the bioactive conformation of 5-HT has yet not been fully characterized, we considered several stable conformers of 5-HT, obtained with the help of quantum chemistry calculations in order to identify 5-HT conformation necessary for uptake by SERT. The optimization procedure and vibrational frequencies calculations, based on the density function theory, indicated the existence of three stable conformers for the 5-HT neurotransmitter (Table 2). They were defined as *anti*, *-gauche* and *+gauche* conformers (Fig. (2) a to c). Here, we applied a systematic approach by superposing all studied compounds on each of the three stable conformers of 5-HT used as rigid templates.

This procedure provided structural models for all tested molecules with a 3D space distribution similar to the 5-HT reference and comparable orientation of the key-functional chemical groups. By this approach, we should have access to the bioactive conformation(s) of each compound transported by SERT.

In addition, this superposition process allowed to precise which chemical groups entered the definition of a pharmacophore of SERT uptake. Structures of seven library compounds, which are SERT-transported with the highest efficiencies, were superposed with 5-HT *anti*, *-gauche*, and *+gauche* conformers (Fig. (2) d to f, respectively). These seven compounds exhibited four important structural determinants: the ammonium group of the ethylamine side

Table 2. Geometries and Relative Energies of the Three Stable Conformers of 5-HT Calculated Using Quantum Chemistry at the B3LYP/6-31+G(d,p) Level of Theory



Conformers	Dihedral angle ^(a)			Relative energy ^(b)
	D ₁	D ₂	D ₃	
<i>+ gauche</i>	-83.742	54.343	-174.782	0
<i>- gauche</i>	-64.395	-49.359	-176.245	0.733
<i>anti</i>	-71.927	172.828	177.777	5.547

(a) Definition of dihedral angles: D₁ = C9-C3-Cβ-Cα, D₂ = C3-Cβ-Cα-N, and D₃ = C4-C5-O-H5.

(b) Relative energy in kcal/mol.

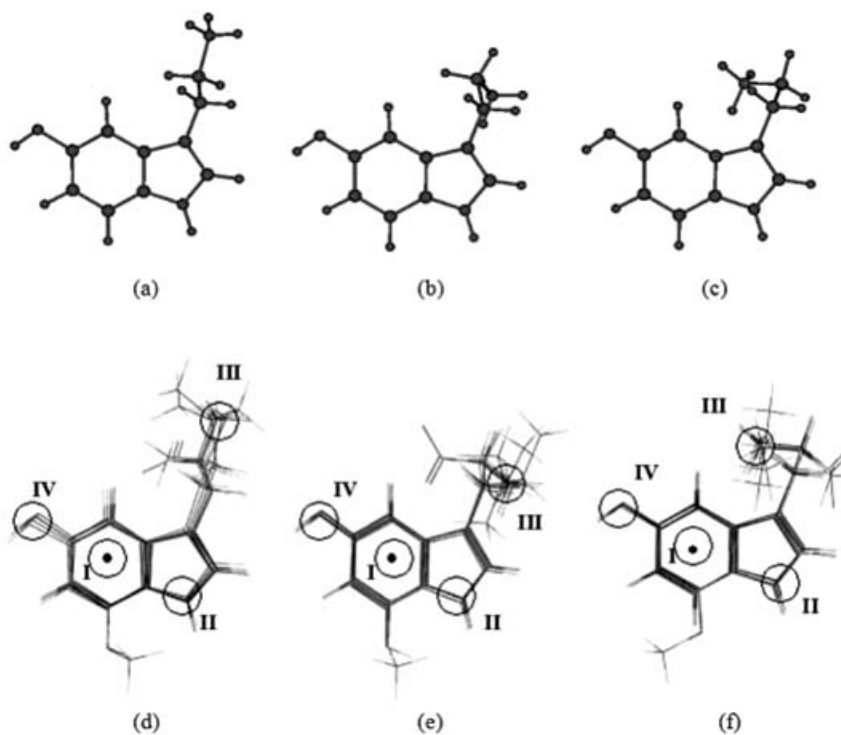


Fig. (2). The three stable conformers of 5-HT (a) *anti*, (b) *-gauche*, and (c) *+gauche* obtained from quantum chemistry calculations at the B3LYP/6-31+G(d,p) level of theory, and the superposition patterns of the seven most active compounds (1-7, Table 1): (d), (e), and (f) correspond to the three stable conformers of 5-HT (a), (b), and (c), respectively. The four pharmacophoric points are indicated; **I** is the aromatic ring center, **II** is the indole nitrogen atom, **III** is the ammonium group of the ethylamine side chain, and **IV** is the oxygen atom of the R₅-OH function.

chain, the R₅ hydroxyl group, the indole nitrogen atom and the phenyl ring center of the indole structure. In combination with SAR data, these modeling results underscore the importance of the above four determinants for a compound to be transported by SERT.

Classical QSAR Analysis

In order to improve the quality of our pharmacophore of SERT activity, we performed a classical QSAR study on 46 analogs of 5-HT. First, 38 descriptors were calculated for each compound using the TSAR3.3 program². Based on the *anti*, *-gauche*, and *+gauche* 5-HT conformers as templates for superposition protocols, PLS analyses generated three classical QSAR models, *i.e.* modI(*t*), modII(*-g*), and modIII(*+g*), for each of the 46 analogs of 5-HT³. The cross-validation of these models using either the LOO or LFO methods clearly indicated that classical QSAR models were not suitable for explaining the relationship between 3D structures and uptake activity of studied compounds.

3D-QSAR Analysis

In order to identify the structural determinant(s) of a molecule important for the uptake by SERT, we first generated 3D molecular interaction fields (MIFs) with DRY, O, and N1 chemical probes used to map the surface of the 46 selected compounds after superposition with the three

reference stable conformers of 5-HT. 3D descriptors

^{2,3}Data available on request.

(GRINDs) were derived from MIFs using the ALMOND program. Although the GRIND approach is not usually superposition dependent [59], we noticed that the results obtained with the three conformers of 5-HT largely differ indicating that superposition protocols are required when considering flexible molecules. 3D GRIND descriptors were then correlated with SERT uptake values leading to 3D-QSAR models.

The first 3D-QSAR models were built without eliminating any descriptors. PLS analysis yielded statistically significant models, modA(*t*), modB(*-g*), and modC(*+g*) corresponding to the *anti*, *-gauche*, and *+gauche* conformers of 5-HT, respectively. The statistical values and optimal parameters for each model are listed in Table 3. The accuracy of our 3D-QSAR models was largely improved, since LFO and LOO cross-validations led to q² ranging from 0.401 to 0.600 and s between 0.428 to 0.524. Five principal components appeared statistically sufficient to describe modA(*t*) and modC(*+g*) models, while a supplementary principal component was necessary to reflect modB(*-g*) model. Using principal components for each model, a conventional non-cross-validation method was carried out leading to r² ranging from 0.894 to 0.911 and s between 0.220 and 0.203.

At this stage, we tried to improve the reliability of derived PLS models. Hence, the fractional factorial design

Table 3. Summary of Statistical Results from PLS Analysis for 3D-QSAR Models Using 46 Compounds of The Training Set Superposed to The Three 5-HT Templates, With and Without FFD Selection of Descriptors

Statistical parameters	Models					
	without FFD			with FFD		
	modA'(t)	modB'(-g)	modC'(g)	modA'(t)	modB'(-g)	modC'(g)
Number of descriptors	185	177	169	133	135	124
q ² _{LOO} ^(a)	0.600	0.447	0.531	0.733	0.695	0.752
s _{LOO} ^(b)	0.428	0.504	0.464	0.350	0.374	0.337
Number of components	5	6	5	5	6	5
q ² _{LFO} ^(c)	0.554	0.401	0.460	0.684	0.650	0.694
s _{LFO} ^(d)	0.452	0.524	0.498	0.381	0.401	0.375
r ² ^(e)	0.911	0.906	0.894	0.930	0.921	0.915
s ^(f)	0.203	0.207	0.220	0.180	0.191	0.198
r ² _{PRED} ^(g)	-	-	-	0.706	-0.809	-0.965
s _{PRED} ^(h)	-	-	-	0.206	0.511	0.532

(a) Leave-one-out (LOO) cross-validation coefficient.

(b) Leave-one-out (LOO) cross-validation standard error of prediction.

(c) Leave-five groups-out (LFO) cross-validation coefficient.

(d) Leave-five groups-out (LFO) cross-validation standard error of prediction.

(e) Non cross-validation (conventional) coefficient.

(f) Non cross-validation (conventional) standard error of estimation.

(g) Correlation coefficient of prediction for external test set, see equation in material and methods.

(h) Standard error of prediction for external test set, see equation in material and methods.

(FFD) variable selection technique was performed for each model. This method allowed to obtain a new PLS model by removing redundant descriptors as well as descriptors that did not significantly contribute to predictability increase. All models with FFD, *i.e.* modA'(t), modB'(-g), and modC'(g), exhibited enhanced predictability (Table 3). q² was enhanced and reached values ranging from 0.650 to 0.752. A q² value above 0.3 is a clear indication of a confidence limit greater than 95%, which suggests that probability of chance correlation is very low (< 5%) [70-71]. In addition, s was lowered and ranged between 0.337 and 0.401. FFD treatment also improved statistics obtained for non-cross-validation for all three models.

Based on FFD-derived models, the ALMOND program calculated for each compound a predictive SERT-uptake value as a combination of all principal components. Correlation plots for 46 compounds between experimental and predicted uptake values calculated for modA'(t), modB'(-g), and modC'(g) are presented in Fig. (3). The results clearly indicate that the most predictive 3D-QSAR model is modA'(t) with the lowest s value of 0.180, while the two other models, modB'(-g) and modC'(g) exhibit s values superior to 0.190.

We next tested the real predictive power of the generated modA'(t), modB'(-g), and modC'(g) models using an external set of compounds, including seven 5-HT analogs (compounds 47 to 53, Table 1), and six substrate-type releasers (Fig. (1)). The latter differs from 5-HT and related analogs by the absence of indole structure. All statistical parameters of external prediction (r²_{PRED}, s_{PRED}), as well as SERT-uptake values predicted for these compounds using

the three models are listed in Table 3 and 4, respectively. Using the external set of compounds, our results firmly establish that predicted SERT uptake values are highly correlated to experimental data only for the modA'(t) model. Accordingly, the s_{PRED} value corresponding to the modA'(t) model (0.206) was significantly lower than the ones of the two other models (0.517 and 0.532). Altogether, our data underscore that the modA'(t) model is the most reliable model to account for SERT uptake. In addition, it is very likely that 5-HT needs to adopt the *anti* conformation to be transported by SERT.

SERT-Uptake Pharmacophore Development

From the modA'(t) 3D-QSAR model, we determined descriptors that were positively and negatively correlated to SERT-uptake values. In this study, we mainly focused on descriptors that were highly positively correlated with uptake, and which were linked to compounds efficiently transported by SERT. Accordingly, close examination of the coefficient plots enabled to select descriptors (Fig. (4), pointed a to h) in each block of node-node interaction, *i.e.* DRY-DRY, O-O, and N1-N1 auto-correlograms, as well as DRY-O, DRY-N1, and O-N1 cross-correlograms. 5-HT was used as the representative molecule to illustrate the largest amplitude of GRINDs, which were positively correlated with SERT uptake in combination with the corresponding molecular interaction field. We deduced that the hydrophobic surface associated to the indole ring confers high affinity binding properties (DRY-DRY distance) to the ligand. We monitored that the six-membered ring of 5-HT is buried into

an hydrophobic pocket belonging to the SERT molecule. This hydrophobic area therefore constitutes a first essential component in our pharmacophore definition of SERT uptake activity. O-O (arrows **b** and **c**) and N1-N1 (arrow **d**) correlograms allowed to define the hydrogen bond network between the 5-HT ligand and SERT residues. In particular, the R₅-OH group and the cationic head and, to a lesser extent, the NH group of the indole ring are crucial protagonists in the establishment of this hydrogen bond network. Distances between each interaction field (*i.e.* hydrophobic and hydrogen bond networks) were estimated from cross-correlograms (DRY-O: arrow **e**, DRY-N1: arrow **f** and O-N1: arrows **g** and **h**), which permitted to precisely define the hindrance of transporting 5-HT through SERT. From these overall data, we were able to refine our pharmacophore definition.

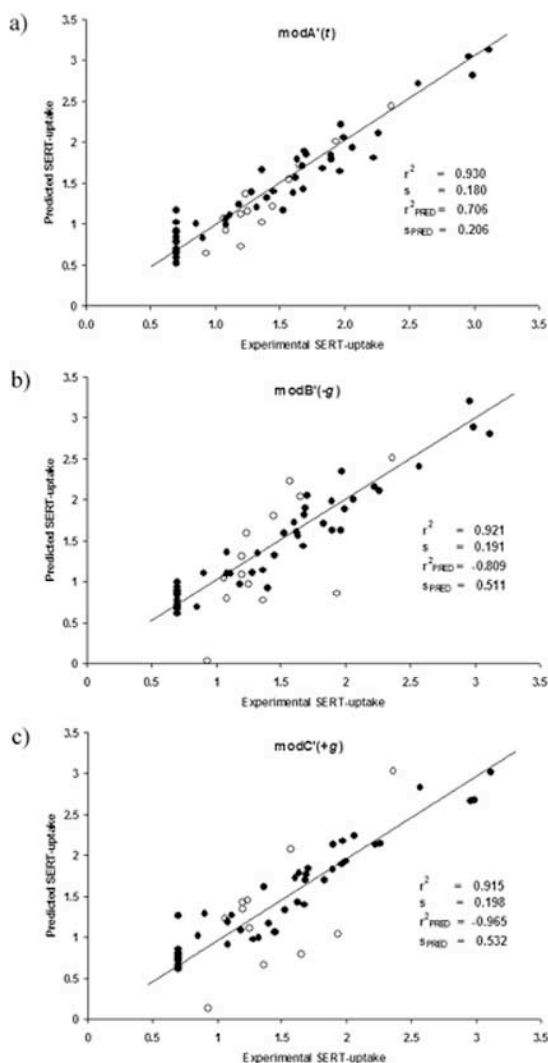


Fig. (3). Correlation of predicted versus experimental SERT-uptake values derived by the PLS analysis models (a) $\text{modA}'(t)$, (b) $\text{modB}'(-g)$, and (c) $\text{modC}'(+g)$. Closed circle represents value of training set and empty circle represents value of external test set.

A 6-point pharmacophore accurately describes geometrical and physicochemical constraints required for efficient 5-HT uptake by SERT (Fig. (5) and Table 5). In this pharmacophore definition, point **I**, which corresponds to

the mass center of the 5-HT phenyl ring, is the center of a hydrophobic sphere delimited by points **V** and **VI**, which are diametrically opposed on an axis perpendicular to the indole ring plane. Points **II** and **III** are representative of two hydrogen bond donor centers and correspond to the nitrogen atom of the indole ring and to the protonated nitrogen of the ethylamine side chain, respectively. Finally, point **IV**, that locates at the R₅ position of the phenyl ring, is involved in the hydrogen bonding of the transported compound either as acceptor or donor of H-bonds depending on the substitution performed at this position.

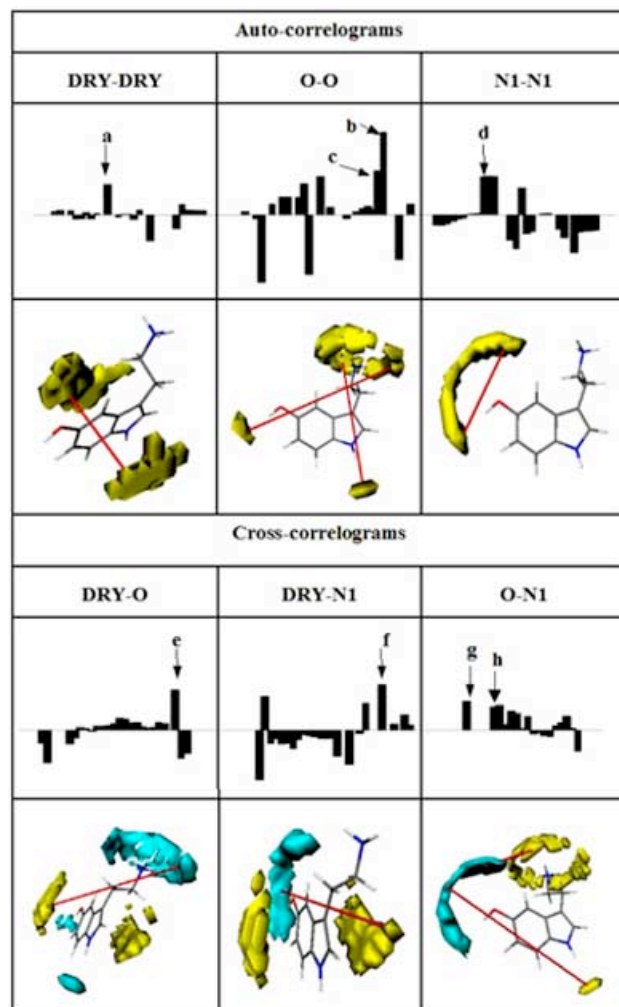


Fig. (4). PLS pseudo-coefficients histogram for $\text{modA}'(t)$ model. Auto-correlograms (DRY-DRY, O-O, and N1-N1) and cross-correlograms (DRY-O, DRY-N1, and O-N1) are both represented. Arrows labelled **a** to **h** indicate the outstanding descriptors with high positive coefficient value corresponding to SERT-uptake activity. The lower part of each correlogram shows the interaction field produced by each probe used to map the surface of 5-HT. The red line indicates the coefficient of GRINDS descriptor corresponding to the upper probe correlograms.

DISCUSSION

Structure-Activity Relationships

Previous SAR studies performed with SERT were not conclusive enough because of the lack of precise conformational analyses of 5-HT and derivatives. This has

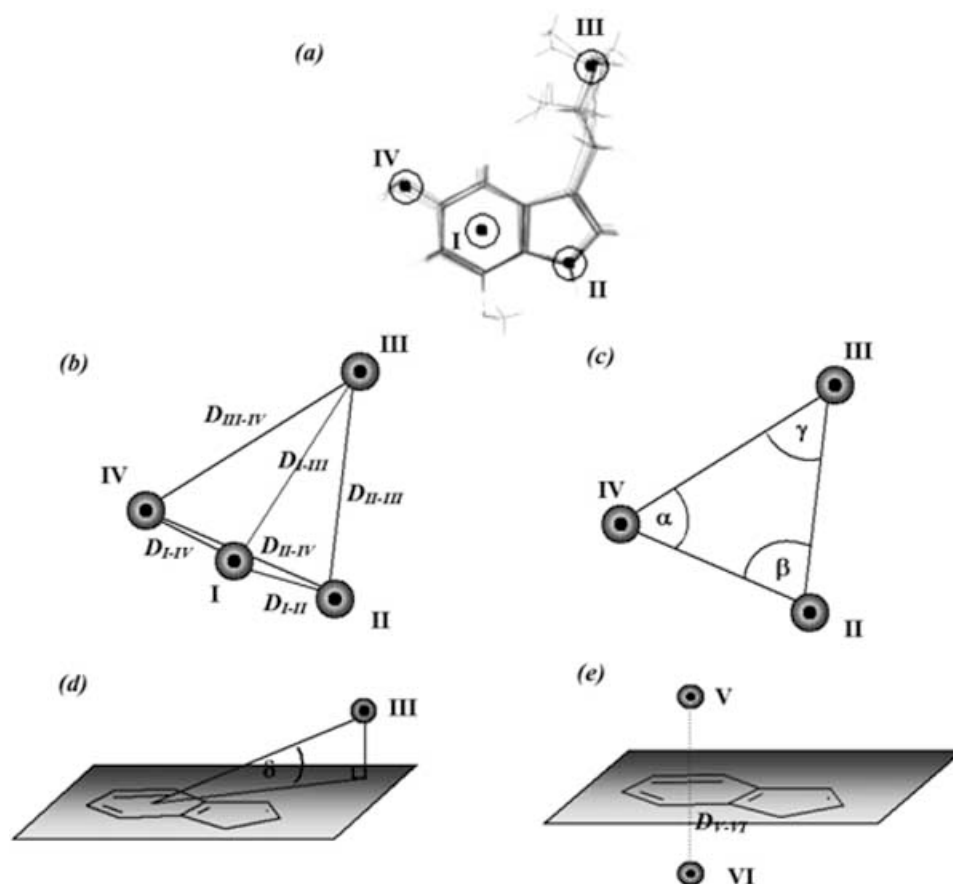


Fig. (5). Graphical representation of the “SERT uptake pharmacophore” model. (a) Superposition of the seven most transported compounds (compound 1-7) using 5-HT *anti* conformer as rigid template. (b) to (e) Detail of pharmacophoric definition; (b) distance between pair of pharmacophoric points; (c) angles between three pharmacophoric points defined as α (II-IV-III), β (III-II-IV), and γ (III-III-IV); (d) δ represents the angle of pharmacophoric point III and the indole plane; and (e) distance between two defined pharmacophoric points, at the upper and lower parts of indole ring plane. Pharmacophoric point I represents hydrophobic interaction and the π -electron delocalisation center of the aromatic indole ring, II represents the hydrogen bond donor center within the indole ring, III represents the hydrogen bond donor and/or electrostatic interaction center of the cationic head side chain; IV represents the hydrogen bond donor and/or acceptor center located on the R₅-hydroxyl group of the indole ring; V and VI represents the center of the hydrophobic field divided upper and lower of the indole ring.

hampered the design of confident pharmacophores representative of SERT uptake activity. For instance, very few reports describe the molecular determinants involved in the interaction between SERT and 5-HT. Nonetheless, the ethylamine side chain of 5-HT, which is protonated at physiological pH, allows the cationic head of the neurotransmitter to interact with a negatively charged residue of the SERT molecule through electrostatic contacts [42]. The amine group of 5-HT is suspected to interact with SERT residues via hydrogen bonds or cation- π contacts based on previous analyses of the binding mode of 5-HT or acetylcholine to their own receptors [67, 69, 72-75].

In this work, we propose a pharmacophore definition of SERT transport that may be useful for the design of new generations of selective drugs. We performed chemical modifications of 5-HT and built a library of 120 analogs. SERT uptake activity was assayed for each compound using human platelets. We demonstrated that the set of generated compounds with no ethylamine side chain are not SERT transported. Furthermore, the introduction of a bulky methyl group in the cationic head (compounds 2 and 4, Table 1), thus augmenting the steric hindrance of this 5-HT side

chain, decreases the uptake capacity of the transporter. The negative impact on the uptake process is also largely correlated to the number of methyl group substitutions. Methyl group introduction at the 5-HT cationic head position generates steric hindrance, which interferes with optimal binding. Moreover, chemical analogs with methyl groups are less flexible than 5-HT, which disfavors salt bridge and/or cation- π interactions with SERT molecule.

Uptake activity with 5-HT-derived compounds where the amine function was substituted by an amide group is also drastically compromised. The acetamide head exhibits a planar configuration and is electroneutral. The amide analog is no more ionizable, which avoids ionic bonding. However, if analog is uptaken, this may reflect the occurrence of electrostatic interactions. The size of the amide group, which also generates steric hindrance, may prevent optimal positioning of 5-HT derivatives bound to SERT.

Addition of a carboxyl group at R _{α} position of the ethylamine side chain (compound 7) significantly decreased uptake of the compound. Since these functional groups (*i.e.* carboxyl and ammonium chemical functions) are very likely

ionized at physiological pH, the strength of the interaction between the derived compound and the SERT molecule should be reinforced as a consequence of multiple salt bridges as compared to 5-HT. On the opposite, such constraint interactions may prevent the correct orientation of the cationic head in the serotonin transporter for an efficient transport. In addition, the presence of a negative charged group at R_α position could be at the origin of repulsive interactions with a negative counterpart on SERT.

The R₅-OH group of 5-HT, which is not protonated at physiological pH, can contribute to neurotransmitter transport through H-bonds with SERT residue(s). The crucial role of the hydroxyl group in 5-HT transport is assessed with compounds **16** and **27** in which the hydroxyl group at the R₅ position is lacking or substituted by a bulkier methoxyl group, respectively. Compounds **16** and **27** are transported by SERT with a huge reduced efficiency. However, we also noticed that R₅ hydroxyl group exchange with a hydrogen atom has less impact on uptake than neutralizing the positive charge at the R_N position (compounds **25**, **80-83**). Those results underline that the presence of the positive charge at the R_N position is a more crucial determinant for SERT uptake activity than the presence of hydroxyl group at R₅ position. Nevertheless, the introduction of a OH group at the R₄ position (compound **13**) partially compensates the absence of R₅ hydroxyl function (compound **16**) regarding SERT-uptake value, while introducing a single OH group at R₆ (compound **15**) or R₇ (compound **14**) positions never improves SERT uptake. We might speculate that the OH group at R₄ position authorizes favorable H-bonds to occur between this functional group and SERT residues. On the opposite, shifting the R₅ hydroxyl group to R₆ or R₇ positions totally impairs H-bond contacts. Moreover, because the replacement of the R₅ hydroxyl group with pure hydrogen bond acceptor functions (compounds **70** and **74**) fully cancels SERT uptake activity, this underscores the role of R₅-OH function as a hydrogen bond donor. Hydroxyl group multi-substitutions at R₅, R₆ and R₇ positions (compounds **6**, **11** and **18**), decrease SERT-uptake activity. This is very likely due to the establishment of a hydrogen bond network between the two or three hydroxyl groups that are simultaneously donor and acceptor of hydrogen bonds. This strong network probably limits the flexibility of R₅ hydroxyl group, thus preventing accommodation of substituted compounds in the SERT binding cleft. Altogether, our results allow to precise how SERT accommodates the 5-HT R₅-OH group. The recognition domain is rather narrow since compounds with bulkier groups are poorly or not transported. This domain favors the selective interaction with the R₅ function, which both behaves as H-bond donor and harbors *sp*³ hybridization. In support with this idea, compound **68** bearing a R₅ group in the *sp*² hybridization state and compound **69** with a non H-bond donor R₅ function are not transported.

The indole ring system is also expected to significantly interact with SERT, either via aromatic-aromatic (stacking or T-shape configuration) or possibly cation- π interactions (cationic head-aromatic interactions) [76-78]. The nitrogen atom included in the indole ring seems to play a major role in the electron distribution throughout the indole ring orbitals, which determines the stability of 5-HT.

Substitution of indole ring nitrogen atom by sulfur or carbon atoms (compounds **8** and **9**, respectively), disturbs the natural 5-HT electron distribution, which in turn interferes with SERT uptake.

At this stage, these biological data reassert the importance of the cationic head, the R₅ hydroxyl group, the indole ring nitrogen atom as well as the aromatic zone of 5-HT for SERT uptake activity. Moreover, we assign specific geometrical and physicochemical properties to each of these four determinants contributing to the first definition of our pharmacophore of SERT transport activity.

Conformational Analysis of Serotonin and Superposition of Compounds

The molecular alignment procedure is an important step in the 3D-QSAR process. The pertinence of the results extracted from the molecule alignment depends on the chosen template. Because any chemical modifications performed on 5-HT affect both the structure and the stability of the derived molecules, we found necessary to investigate 5-HT conformation. This study is a prerequisite before performing 3D-QSAR analysis since 5-HT may adopt multiple conformations. 5-HT conformational analysis was performed using quantum chemistry calculations. 5-HT conformers with *+gauche*, *-gauche* and *anti* conformation were found as the most stable isomers. In those isomers, the flexibility of the 5HT cationic side chain largely depends on the electron distribution over the molecule. The existence of these three energy minima relates to the repartition of charges within the indole ring, which is influenced by the presence of the R₅ hydroxyl group and the indole ring nitrogen atom.

3D-QSAR Analysis

Because the predictive power of our classical QSAR models to characterize SERT uptake activity does not satisfy the statistical significance (see results), we have built a 3D-QSAR model to correctly describe the relationship between compound structures and their ability to be SERT transported. The failure in obtaining a reliable model for SERT transport activity through the use of classical QSAR protocols is related to descriptors that do not include 3D parameters. In particular, the electron distribution within the 5-HT molecule as indicated by quantum chemistry calculations largely influences the flexibility and spatial orientation of the 5-HT cationic side chain, partly supporting the bioactivity of 5-HT. To overcome this limitation, QSAR models built with the help of 3D descriptors enable to fully characterize the relationship between compound structures and SERT transport activities. We thus generated three 3D-QSAR models using the *anti*, *+gauche* and *-gauche* conformers of 5-HT as templates. GRINDs were extracted from interaction field vectors surrounding the aligned molecules and PLS analyses were carried out. For each of the three 5-HT conformers, a 3D-QSAR model was derived (see Table 3). All models exhibited largely improved statistical significance as compared to classical QSAR models with higher *q*² and lower *s* values whatever the cross-validation method used, or with enhanced *r*² in non cross-validation procedures. These results argue that

Table 4. Experimental and Predicted SERT-uptake Values of External Test Set Performed Using Three PLS Models: modA'(t), modB'(-g), and modC'(+g)

Compound	SERT-uptake (nmole/10 ⁹ platelets)			
	Experimental	Prediction		
		modA'(t)	modB'(-g)	modC'(+g)
<i>5-HT analogs</i>				
47	2.30 ± 0.02	2.75	3.31	10.72
49	0.37 ± 0.09	0.35	1.70	1.20
50	0.28 ± 0.02	0.16	0.63	0.12
51	0.23 ± 0.03	0.15	0.06	0.05
48	0.84 ± 0.07	1.02	0.07	0.11
52	0.17 ± 0.06	0.23	0.39	0.28
53	0.16 ± 0.04	0.05	0.12	0.26
<i>Substrate-type 5-HT releasing agents</i>				
amphetamine	0.16 ± 0.05	0.13	0.20	0.22
fenfluramine	0.18 ± 0.03	0.15	0.09	0.13
norfenfluramine	0.12 ± 0.01	0.08	0.06	0.16
phentermine	0.12 ± 0.02	0.12	0.11	0.17
HMMA	0.45 ± 0.05	0.53	1.10	0.06
TFMPP	0.09 ± 0.02	0.04	0.01	0.01

including 3D descriptors in the building process is of priority to improve the reliability of the QSAR model for SERT activity.

Table 5. Pharmacophoric Parameters Corresponding to Pharmacophoric Points Shown in Fig. (5)

Pharmacophoric components	Mean ± SD (unit)
<i>Distance</i>	(<i>Å</i>)
D _{I-II}	2.75 ± 0.02
D _{I-III}	5.78 ± 0.11
D _{I-IV}	2.77 ± 0.02
D _{II-III}	5.89 ± 0.06
D _{II-IV}	5.51 ± 0.01
D _{III-IV}	6.60 ± 0.26
D _{I-V}	3.29 ± 0.20
D _{I-VI}	3.40 ± 0.20
D _{V-VI}	6.54 ± 0.20
<i>Angle</i>	(<i>°</i>)
α	57.39 ± 2.23
β	70.70 ± 3.59
γ	51.91 ± 1.44
δ	14.83 ± 1.32

The use of indole and substrate-type releaser derivatives as external test set compounds (see Table 4) enable to define

the modA'(t) model, which is derived from the 5-HT *anti* conformer, as to be the most appropriate 3D-QSAR model to account for the biological activity of SERT. This is supported by the lowest statistical value of standard error of prediction (s_{PRED}) and the highest correlation coefficient of prediction (r²_{PRED}) as the result of the smallest dispersion of data points in correlation profiles between experimental and predictive transport values (see Table 3 and Fig. (3)). These results highlight that the bioactive conformation of 5-HT adapted for SERT transport is very likely the *anti* conformation. However, it is interesting to note from our quantum chemistry calculations that the *anti* conformation does not correspond to the 5-HT molecule with the global energy minimum. Our data suggest that the conformational energy of compounds transported by SERT does not represent a key factor for SERT uptake. Nevertheless, we cannot exclude that such conformers in biological fluids are recognized by SERT and that 5-HT conformation changes along the translocation process inside SERT.

To conclude, the identification of the 5-HT *anti* conformation as the biological active form toward SERT transport has strong implications for the definition of the pharmacophore of SERT uptake activity.

Pharmacophore Development

Our pharmacophore definition of SERT uptake activity relies on the identification of six pharmacophoric determinants from interaction field analyses and QSAR studies (Fig. (5)). This pharmacophore is built based on the

seven most transported compounds, which interact with SERT in a similar manner. Our SERT pharmacophore uptake model allows to appreciate the steric hindrance and volume of SERT-transported compounds through the precise calculation of distances between each couple of pharmacophoric key-points and angle values between three pharmacophoric determinants. Since all distances associated to each pharmacophoric component doublet are comprised between 2.75 Å and 6.60 Å, we conclude that the shape of the pharmacophore is rather compact. This gives some clues as to the tightness of the volume occupied by 5-HT or derivatives. The importance of (i) the number of fitting pharmacophoric points, (ii) the geometrical constraints (distances and angles) and (iii) the spatial distribution of virtual interacting points within the transporter, was evaluated through the analysis of structures superposed on the pharmacophoric pattern of highly (compound 2-7), moderately (compound 15), poorly (compound 24) and non transported (compound 44) compounds (Fig. (6)). HMMA, which belongs to the external test set is also represented and corresponds to a moderately SERT transported compound. Consistent with our pharmacophore definition, none of the tested analogs, except compound 2-7, fulfills the requirement of pharmacophore components for uptake. With

highly and moderately transported compounds 2-7 and 15, respectively, the number of matching pharmacophoric points still equals 6. The topology of the putative SERT binding pocket is similar for compound 2-7 as compared to 5-HT *anti* conformer. With compound 15, the six-pharmacophoric components do not exactly match the 3D space arrangement of 5-HT, since the position of the hydrogen bond donor and/or acceptor point IV is shifted to position R₆. In this case, such orientation of the R₆ group does not favor interactions with SERT residues. Concerning the poorly transported compound 24, the huge decrease in uptake value can be explained by the loss of pharmacophoric point IV. With compound 44, the absence of uptake property is due to the loss of pharmacophoric point III. This is also the case for all compounds that lack nitrogen atom in the ethylamine side chain. By contrast, superposition of HMMA on 5-HT reveals similarities between indolic and non-indolic compounds, *i.e.* spatial arrangement and specific contacts with SERT. A good fit of HMMA with 4 on the 6 pharmacophoric points associated with a partial overlap of the hydrophobic volume, do explain its moderate uptake.

To summarize, our overall data illustrate that all of the six points of the pharmacophore are critical to sustain SERT

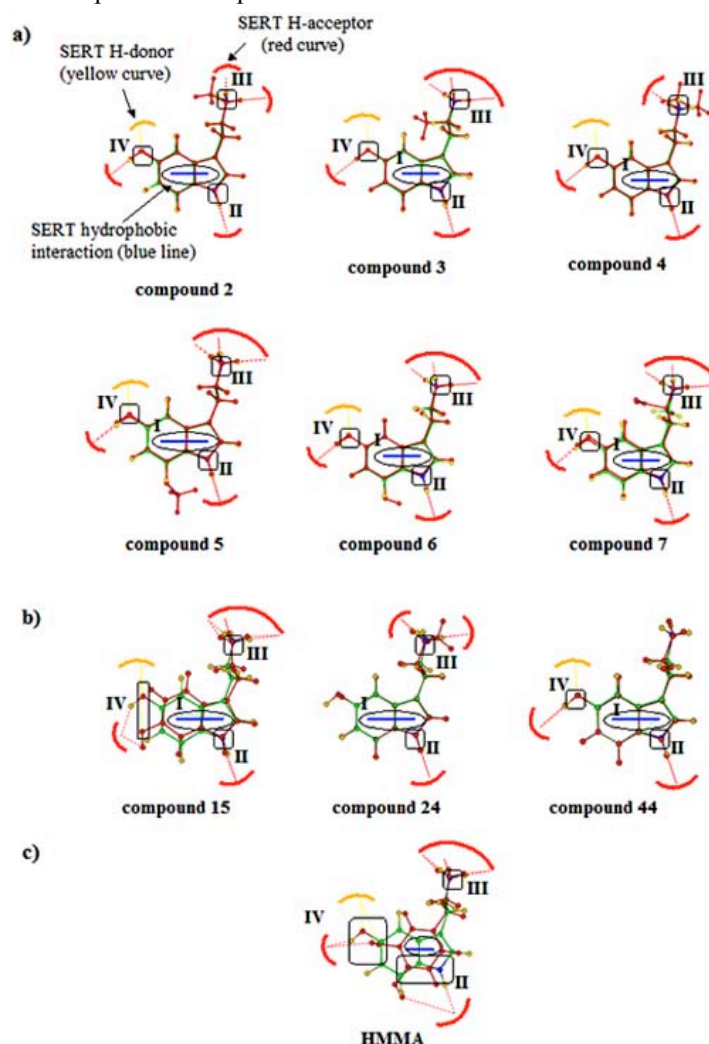


Fig. (6). Alignment of **a)** efficiently transported compounds (compounds 2 to 7), **b)** moderately, poorly, and non-transported compounds (compounds 15, 24, and 44, respectively) and **c)** external tested compound HMMA with 5-HT *anti* conformer to pinpoint fitting interaction points between those molecules and our explanatory pharmacophore model.

uptake activity. All results support the view that any modification of only one of the six determinants alters SERT transport. However, each pharmacophoric point does not equally contribute to SERT transport activity. The effect on compound uptake largely depends on the pharmacophoric point affected by the chemical modification. Alternate substitution of components **III** and **IV** drastically impacts on uptake, while modification of all other determinants is less detrimental. Interestingly, quantum chemistry and QSAR study have shown that component **II** weakly participates to a direct interaction with SERT through H-bond, but rather participates to the stabilization of the pharmacophore by influencing electron distribution within the 5-HT molecule. The hydrophobic volume defined by pharmacophoric points **I**, **V** and **VI**, largely determines SERT uptake capacity. Nevertheless, substrate-type releaser molecules partially overlap this hydrophobic volume, which authorizes the molecules to be transported by SERT.

In order to control the validity of our pharmacophore, we analyzed the conformation distribution of 46 compounds that we used to design our SERT uptake pharmacophore. Compounds **2-7**, **15**, **24** and **44** shown in Fig. (6) are representative of molecules that are efficiently, moderately, poorly and non-transported, respectively. Although tested molecules were always considered flexible in our modeling experiments, the alignment process never controlled the reliability of the selected conformations. To overcome this limitation, MD analyses enabled to calculate the percentage of molecules harboring an *anti* conformation, since this conformation is supposed to be the bioactive form of 5-HT.

From 5-HT MD simulations, the *anti* conformer represents 10% of all the probable 5-HT conformers, despite a high energy level as compared to the *+gauche* and *-gauche* conformers. The existence of two real transition states allows 5-HT with the *anti* conformation to be trapped in a potential well. Because the energy barriers that permit 5-HT conformation to evolve from the *+gauche* or *-gauche* conformations to the *anti* form are probably not so high, the population size of 5-HT with the *anti* conformation is statistically significant. This favors the hypothesis that a minimum of energy is required for SERT to impose the *anti* conformation to the transporting 5-HT. With compound **7**, which is one of the tested molecules the most efficiently uptaken by SERT, the population size of compound **7** with the *anti* conformation equals 6%. This percentage drops down to 1.2% and 0.5% when considering poorly and non-transported compounds **27** and **46**, respectively.

CONCLUSION

For the first time, we design a six-determinant pharmacophore that relates to SERT uptake activity. All chemically modified compounds transported by SERT adopt similar conformation to the one of 5-HT, which we find as to be the *anti* form. Our combined approaches of quantum chemistry and 3D-QSAR analyses enable to generate a high confident pharmacophore for SERT transport activity (*i.e.* with non-cross-validation r^2 of 0.930, internal cross validation q^2_{LOO} and q^2_{LFO} of 0.733 and 0.684, respectively). This pharmacophore may provide new informations regarding mechanisms of compound transport

through the serotonin transporter and may be useful for the building of structural models of SERT. Besides, a major priority in 5-HT-associated demises (schizophrenia, obsession compulsive disorders, treatment of mood, ...) is to introduce in therapeutic protocols new generations of molecules that efficiently target SERT. Indeed, we are convinced that a reliable descriptor of SERT transport could be derived from our pharmacophore model and may provide a useful tool to evaluate how much a compound fits the pharmacophore and to predict its biological activity.

ACKNOWLEDGEMENTS

This study was partially supported by BioQuanta *Inside cell* Corp, CO, USA.

REFERENCES

- [1] Hoyer, D.; Hannon, J.P.; Martin, G.R. *Pharmacol. Biochem. Behav.*, **2002**, *71*, 533.
- [2] Blakely, R.D.; De Felice, L.J.; Hartzell, H.C. *J. Exp. Biol.*, **1994**, *196*, 263.
- [3] Uhl, G.R.; Johnson, P.S. *J. Exp. Biol.*, **1994**, *196*, 229.
- [4] Rudnick, G.; Clark, J. *Biochim. Biophys. Acta.*, **1993**, *1144*, 249.
- [5] Rothman, R.B.; Baumann, M.H. *Eur. J. Pharmacol.*, **2003**, *479*, 23.
- [6] Rothman, R.B.; Baumann, M.H. *Pharmacol. Ther.*, **2002**, *95*, 73.
- [7] Nelson, N. *J. Neurochem.*, **1998**, *71*, 1785.
- [8] Sur, C.; Betz, H.; and Schloss, P. *Proc. Natl. Acad. Sci. USA*, **1997**, *94*, 7639.
- [9] Barker, E.L.; Blakely, R.D. *Mol. Pharmacol.*, **1996**, *50*, 957.
- [10] Chen, J.G.; Sachpatzidis, A.; Rudnick, G. *J. Biol. Chem.*, **1997**, *272*, 28321.
- [11] Barker, E.L.; Perlman, M.A.; Adkins, E.M.; Houlihan, W.J.; Pristupa, Z.B.; Niznik, H.B.; Blakely, R.D. *J. Biol. Chem.*, **1998**, *273*, 19459.
- [12] Cao, Y.; Li, M.; Mager, S.; Lester, H.A. *J. Neurosci.*, **1998**, *18*, 7739.
- [13] Chen, J.G.; Liu-Chen, S.; Rudnick, G. *J. Biol. Chem.*, **1998**, *273*, 12675.
- [14] Penado, K.M.; Rudnick, G.; Stephan, M.M. *J. Biol. Chem.*, **1998**, *273*, 28098.
- [15] Barker, E.L.; Moore, K.R.; Rakhshan, F.; Blakely, R.D. *J. Neurosci.*, **1999**, *19*, 4705.
- [16] Smicun, Y.; Campbell, S.D.; Chen, M.A.; Gu, H.; Rudnick, G. *J. Biol. Chem.*, **1999**, *274*, 36058.
- [17] Chen, J.G.; Rudnick, G. *Proc. Natl. Acad. Sci. USA*, **2000**, *97*, 1044.
- [18] Adkins, E.M.; Barker, E.L.; Blakely, R.D. *Mol. Pharmacol.*, **2001**, *59*, 514.
- [19] Androutsellis-Theotokis, A.; Ghassemi, F.; Rudnick, G. *J. Biol. Chem.*, **2001**, *276*, 45933.
- [20] Kamdar, G.; Penado, K.M.; Rudnick, G.; Stephan, M.M. *J. Biol. Chem.*, **2001**, *276*, 4038.
- [21] Mortensen, O.V.; Kristensen, A.S.; Wiborg, O. *J. Neurochem.*, **2001**, *79*, 237.
- [22] Androutsellis-Theotokis, A.; Rudnick, G. *J. Neurosci.*, **2002**, *22*, 8370.
- [23] Henry, L.K.; Adkins, E.M.; Han, Q.; Blakely, R.D. *J. Biol. Chem.*, **2003**, *278*, 37052.
- [24] Kilic, F.; Murphy, D.L.; Rudnick, G. *Mol. Pharmacol.*, **2003**, *64*, 440.
- [25] Kristensen, A.S.; Larsen, M.B.; Johnsen, L.B.; Wiborg, O. *Eur. J. Neurosci.*, **2004**, *19*, 1513.
- [26] Larsen, M.B.; Elfving, B.; Wiborg, O. *J. Biol. Chem.*, **2004**, *279*, 42147.
- [27] Mitchell, S.M.; Lee, E.; Garcia, M.L.; Stephan, M.M. *J. Biol. Chem.*, **2004**, *279*, 24089.
- [28] Edvardsen, O.; Dahl, S.G. *Brain Res. Mol. Brain Res.*, **1991**, *9*, 31.
- [29] Ravna, A.W.; Edvardsen, O. *J. Mol. Graph. Model*, **2001**, *20*, 133.
- [30] Ravna, A.W.; Sylte, I.; Dahl, S.G. *J. Comput. Aid. Mol. Des.*, **2003**, *17*, 367.

- [31] Ravna, A.W.; Sylte, I.; Dahl, S.G. *J. Pharmacol. Exp. Ther.*, **2003**, 307, 34.
- [32] Williams, K.A. *Nature*, **2000**, 403, 11.
- [33] Baumgarten, H.G.; Bjorklund, A.; Nobin, A.; Rosengren, E.; Schlossberger, H.G. *Acta Physiol. Scand. Suppl.*, **1975**, 429, 5.
- [34] Bjorklund, A.; Horn, A.S.; Baumgarten, H.G.; Nobin, A.; Schlossberger, H.G. *Acta Physiol. Scand. Suppl.*, **1975**, 429, 29.
- [35] Horn, A.S. *J. Neurochem.*, **1973**, 21, 883.
- [36] Horn, A.S. *Ann. NY Acad. Sci.*, **1978**, 305, 128.
- [37] Chang, A.S.; Chang, S.M.; Starnes, D.M. *Eur. J. Pharmacol.*, **1993**, 247, 239.
- [38] Wang, S.; Sakamuri, S.; Enyedy, I.J.; Kozikowski, A.P.; Deschoux, O.; Bandyopadhyay, B.C.; Tella, S.R.; Zaman, W.A.; Johnson, K.M. *J. Med. Chem.*, **2000**, 43, 351.
- [39] Enyedy, I.J.; Zaman, W.A.; Sakamuri, S.; Kozikowski, A.P.; Johnson, K.M.; Wang, S. *Bioorg. Med. Chem. Lett.*, **2001**, 11, 1113.
- [40] Enyedy, I.J.; Sakamuri, S.; Zaman, W.A.; Johnson, K.M.; Wang, S. *Bioorg. Med. Chem. Lett.*, **2003**, 13, 513.
- [41] Wellsov, J.; Machulla, H.-J.; Kovar, K.-A. *Quant. Struct.-Act. Relat.*, **2002**, 21, 577.
- [42] Appell, M.; Dunn III, W.J.; Reith, M.E.A.; Miller, L.; Flippen-Anderson, J.L. *Bioorg. Med. Chem.*, **2002**, 10, 1197.
- [43] Omenn, G.S.; Smith, L.T. *J. Clin. Invest.*, **1978**, 62, 235.
- [44] Lesch, K.P.; Wolozin, B.L.; Murphy, D.L.; Reiderer, P. *J. Neurochem.*, **1993**, 60, 2319.
- [45] Soliman, H.R.; Oset-Gasque, M.J.; Callebert, J.; Launay J.M.; Tabuteau, F.; Dreux, C. *Thromb. Res.*, **1987**, 45, 279.
- [46] Launay, J.M.; Geoffroy, C.; Mutel, V.; Buckle, M.; Cesura, A.; Alouf, J.E.; Da Prada, M. *J. Biol. Chem.*, **1992**, 267, 11344.
- [47] Gadd, R.E.A.; Clayman, S. *Experientia*, **1972**, 28, 719.
- [48] Lemasson, M.H.; Bonnet, J.J.; Costentin, J. *Biochem. Pharmacol.*, **1984**, 33, 2137.
- [49] Brooks, B.R.; Bruccoleri, R.E.; Olafson, B.D.; States, D.J.; Swaminathan, S.; Karplus, M. *J. Comput. Chem.*, **1983**, 4, 187.
- [50] Chattopadhyay, A.; Rukmini, R.; Mukherjee, S. *Biophys. J.*, **1996**, 71, 1952.
- [51] Jorgensen, W.L.; Chandrasekhar, J.D.; Madura, R.W.; Impey, R.W.; Klein, M.L. *J. Chem. Phys.*, **1983**, 79, 926.
- [52] Ryckaert, J.P.; Ciccotti, G.; Berendsen, H.C. *J. Comp. Phys.*, **1977**, 23, 327.
- [53] Frisch, M.J.; Trucks, G.W.; Schlegel, H.B.; Scuseria, G.E.; Robb, M.A.; Cheeseman, J.R.; Montgomery, Jr., J.A.; Vreven, T.; Kudin, K.N.; Burant, J.C.; Millam, J.M.; Iyengar, S.S.; Tomasi, J.; Barone, V.; Mennucci, B.; Cossi, M.; Scalmani, G.; Rega, N.; Petersson, G. A.; Nakatsuji, H.; Hada, M.; Ehara, M.; Toyota, K.; Fukuda, R.; Hasegawa, J.; Ishida, M.; Nakajima, T.; Honda, Y.; Kitao, O.; Nakai, H.; Klene, M.; Li, X.; Knox, J.E.; Hratchian, H.P.; Cross, J.B.; Bakken, V.; Adamo, C.; Jaramillo, J.; Gomperts, R.; Stratmann, R.E.; Yazyev, O.; Austin, A.J.; Cammi, R.; Pomelli, C.; Ochterski, J.W.; Ayala, P.Y.; Morokuma, K.; Voth, G.A.; Salvador, P.; Dannenberg, J.J.; Zakrzewski, V.G.; Dapprich, S.; Daniels, A.D.; Strain, M.C.; Farkas, O.; Malick, D.K.; Rabuck, A.D.; Raghavachari, K.; Foresman, J.B.; Ortiz, J.V.; Cui, Q.; Baboul, A.G.; Clifford, S.; Cioslowski, J.; Stefanov, B.B.; Liu, G.; Liashenko, A.; Piskorz, P.; Komaromi, I.; Martin, R.L.; Fox, D.J.; Keith, T.; Al-Laham, M.A.; Peng, C.Y.; Nanayakkara, A.; Challacombe, M.; Gill, P. M.W.; Johnson, B.; Chen, W.; Wong, M.W.; Gonzalez, C.; and Pople, J.A.; Gaussian, Inc., Wallingford CT, **2004**.
- [54] Lemmen, C.; Lengauer, T.; Klebe, G. *J. Med. Chem.*, **1998**, 41(23), 4502.
- [55] Lemmen, C.; Lengauer, T. *J. Comput. Aided Mol. Des.*, **1997**, 11(4), 357.
- [56] Lemmen, C.; Hiller, C.; Lengauer, T. *J. Comput. Aid. Mol. Des.*, **1998**, 12(5), 491.
- [57] Lemmen, C.; Lengauer, T. *J. Comput. Aided Mol. Des.*, **2000**, 14(3), 215.
- [58] Cruciani, G.; Watson, K.A. *J. Med. Chem.*, **1994**, 37, 2589.
- [59] Baroni, M.; Costantino, G.; Cruciani, G.; Riganelli, D.; Valigi, R.; Clementi, S. *Quant. Struct. Act. Relat.*, **1993**, 12, 9.
- [60] Murthy, S.V.; Kulkarni V.M. *Bioorg. Med. Chem.*, **2002**, 10, 2267.
- [61] Pastor, M.; Cruciani, G.; Clementi, S. *J. Med. Chem.*, **1997**, 40, 1455.
- [62] Pastor, M.; Cruciani, G.; Watson, K.A. *J. Med. Chem.*, **1997**, 40, 4089.
- [63] Sippl, W. *J. Comput. Aid. Mol. Des.*, **2000**, 14, 559.
- [64] Sippl, W.; Contreras, J.M.; Parrot, I.; Rival, Y.M.; Wermuth, C.G. *J. Comput. Aid. Mol. Des.*, **2001**, 15, 395.
- [65] Pastor, M.; Cruciani, G.; McLay, I.; Pickett, S.; Clementi, S. *J. Med. Chem.*, **2000**, 43, 3233.
- [66] Ho, B.Y.; Karschin, A.; Branchek, T.; Davidson, N.; Lester, H.A. *FEBS Lett.* **1992**, 312, 259.
- [67] Wang, C.D.; Gallaher, T.K.; Shin, J.C. *Mol. Pharmacol.*, **1993**, 43, 931.
- [68] Kristiansen, K.; Kroeze, W.K.; Willins, D.L.; Gelber, E.I.; Savage, J.E.; Glennon, R.A.; Roth, B.L. *J. Pharmacol. Exp. Ther.*, **2000**, 293, 735.
- [69] Manivet, P.; Schneider, B.; Smith, J.C.; Choi, D.S.; Maroteaux, L.; Kellermann, O.; Launay, J.M. *J. Biol. Chem.*, **2002**, 277, 17170.
- [70] Clark, M.; Cramer III, R.D. *Quant. Struct.-Act. Relat.*, **1993**, 12, 137.
- [71] Kaminski, J.J.; Doweiko, A.M. *J. Med. Chem.* **1997**, 40, 427.
- [72] Edvardsen, O.; Sylte, I.; Dahl, S.G. *Brain Res. Mol. Brain Res.*, **1992**, 14, 166.
- [73] Dougherty, D. A. *Science*, **1996**, 271, 163.
- [74] Zhong, W.; Gallivan, J.P.; Zhang, Y.; Li, L.; Lester, H.A.; Dougherty, D.A. *Proc. Natl. Acad. Sci. USA*, **1998**, 95, 12088.
- [75] Beene, D.L.; Brandt, G.S.; Zhong, W.; Zacharias, N.M.; Lester, H.A.; Dougherty, D.A. *Biochemistry*, **2002**, 41, 10262.
- [76] Burley, S.K.; Petsko, G.A. *Adv. Protein Chem.*, **1988**, 39, 125.
- [77] Levitt, M.; Perutz, M.F. *J. Mol. Biol.*, **1988**, 201, 751.
- [78] Singh, J.; Thornton, J.M. *J. Mol. Biol.*, **1990**, 211, 595.

Copyright of Current Medicinal Chemistry is the property of Bentham Science Publishers Ltd.. The copyright in an individual article may be maintained by the author in certain cases. Content may not be copied or emailed to multiple sites or posted to a listserv without the copyright holder's express written permission. However, users may print, download, or email articles for individual use.